

Acoustic energy relations in Mudejar-Gothic churches

Teófilo Zamarreño,^{a)} Sara Girón,^{b)} and Miguel Galindo^{c)}

*Departamento de Física Aplicada II, Universidad de Sevilla, ETS de Arquitectura IUCC,
Avda. Reina Mercedes 2, 41012-Sevilla, Spain*

(Received 3 February 2006; revised 11 October 2006; accepted 14 October 2006)

Extensive objective energy-based parameters have been measured in 12 Mudejar-Gothic churches in the south of Spain. Measurements took place in unoccupied churches according to the ISO-3382 standard. Monoaural objective measures in the 125–4000 Hz frequency range and in their spatial distributions were obtained. Acoustic parameters: clarity C_{80} , definition D_{50} , sound strength G and center time T_5 have been deduced using impulse response analysis through a maximum length sequence measurement system in each church. These parameters spectrally averaged according to the most extended criteria in auditoria in order to consider acoustic quality were studied as a function of source-receiver distance. The experimental results were compared with predictions given by classical and other existing theoretical models proposed for concert halls and churches. An analytical semi-empirical model based on the measured values of the C_{80} parameter is proposed in this work for these spaces. The good agreement between predicted values and experimental data for definition, sound strength, and center time in the churches analyzed shows that the model can be used for design predictions and other purposes with reasonable accuracy. © 2007 Acoustical Society of America. [DOI: 10.1121/1.2390665]

PACS number(s): 43.55.Br, 43.55.Gx [NX]

Pages: 234–250

I. INTRODUCTION

The study of the sound field in places of worship, in any type of religion and both for new buildings and for rehabilitation of ancient existing buildings (patrimony preservation), has recently aroused great interest within the general field of architectural acoustics as is evident from the research literature,^{1–3} from some of the latest international congresses such as in Rome⁴ and Seville (Spain),⁵ which featured a specific session for worship building acoustics, and from other related projects.⁶ On one hand, this interest is of a practical nature as a result of the growing demand for acoustic comfort in public places which are used for oral or musical liturgical purposes or for other cultural performances. On the other hand, the interest is more fundamental since the investigation into the acoustics of these complex spaces gives information about the general acoustic aspects of architectural heritage and aids the general comprehension of room acoustics.

This paper deals with the experimental results of certain monoaural energy-based acoustic parameters: clarity, definition, sound strength, and center time, all studied as a function of source-receiver distance, and proposes a model to interpret such experimental data. These parameters are considered very relevant for the evaluation of acoustic quality based on energy criteria. The parameters have been measured for octave bands between 125 and 4000 Hz and within their spatial distribution in each church. In the present analysis each parameter has been averaged spectrally in accordance with the most widely accepted way.

From the starting point of the deviation of the ideal pattern of a diffuse sound field in these places as shown by all the parameters analyzed and the comparison of the experimental data with the revised theory of Barron *et al.*⁷ for concert halls, the semiempirical model deduced from the experimental sound pressure values, proposed by Sendra *et al.*⁸ for these types of religious spaces and the modified theory of Cirillo *et al.*,⁹ originally conceived for Romanesque churches and recently refined to include a wider type of churches,¹⁰ have led the authors¹¹ to propose a relatively simple model based on measured C_{80} values. Hence, with volume, reverberation time, source-receiver distances and μ parameter as premises, this model enables the prediction of all the remaining measured acoustic parameters studied in churches of this character in the south of Spain. These churches constitute an important sample of the cultural inheritance of the city which had a strong influence on Latin American Baroque architecture which includes the Mudejar timber roofs in important churches in Columbia, Bolivia, El Salvador and Cuba.

II. MEASUREMENT TECHNIQUE

The procedures employed have been those established in the ISO-3382 standard and all measures have been carried out in unoccupied churches. Temperature and relative humidity have been measured with a precision electronic thermohygrometer and a barometer has determined the atmospheric pressure. The range of variation was 22.6–27.4 °C for the temperature, 35.7–65.7% for the relative humidity, and 101.7–102.5 kPa for the atmospheric pressure.

Monoaural impulse responses and other room responses to stationary signals have been measured to determine reverberation times (T) together with the energy-based parameters for each frequency band in all receiver positions: clarity (C_{80}), definition (D_{50}), sound strength (G) and center time

^{a)}Electronic mail: teofilo@us.es

^{b)}Electronic mail: sgron@us.es

^{c)}Electronic mail: mgalindo@us.es

(T_S). From this point on, these parameters are spectrally averaged in each position as follows: clarity and center time as a direct average of 500, 1000, and 2000 Hz octave band values, definition as a weighted average in the same way as Marshall¹² proposed for C_{50} :

$$D_{50av} = 0.15D_{50}(500 \text{ Hz}) + 0.25D_{50}(1 \text{ kHz}) + 0.35D_{50}(2 \text{ kHz}) + 0.25D_{50}(4 \text{ kHz}) \quad (1)$$

and a mean of the corresponding mid-frequency 500 and 1000 Hz bands for sound strength¹³ and reverberation time.

The impulse response has been obtained using maximum length sequence (MLS) signals. The analyzer used has been the Maximum Length Sequence System Analyzer, from DRA Laboratories (MLSSA) based on a full-length Industry Standard Architecture (ISA) card of data acquisition housed in a slot of a PC with the corresponding software which runs under MS-DOS operating system. For the measurement of the impulse response in order to obtain the decay curves and the energy parameters, the MLS spectrum must be conditioned to that of pink noise before being fed to the amplifier. This is done here by means of the CWF-1 filter from One-on-One Technical Products. In order to improve the signal-to-noise ratio at low frequencies, the signal captured by the microphone is inverse filtered before entering MLSSA for its analysis. In addition, to improve this signal-to-noise ratio, in each position, the impulse response is obtained by averaging eight MLS periods.

An omnidirectional source B&K 4296 is placed at the most usual point of location of the natural source: the altar at a height of 1.70 m from the floor. The microphone is located at the approximate height of the head of a seated person which is 1.20 m from the floor, in a predetermined number of positions distributed in the central nave and the lateral naves ranging from 12 reception points of Santa Catalina church to 23 of Santa Marina (see Fig. 1).

The microphone used is a 1/2 in. B&K 4190, and a B&K 2669 preamplifier and a bias-source B&K 2804, to supply the 200 V dc polarization voltage necessary.

In order to study sound pressure levels, two different techniques for the calculation of sound strength have been used. The first technique uses the emission of a stationary signal, later corrected with the level produced by the source, at 10 m distance under free field conditions. The other technique is derived from the impulse response generated from the MLS signals, by means of calculating the reference level from the direct sound of this impulse response and from its source-receiver distance. This distance is calculated from the initial flying time of the impulse responses. The results coming from these two techniques have been compared through lineal regression and a slope near to one has been obtained: $y=0.962x$; $R^2=0.824$. The coefficient of the determination is acceptable if one takes into account that the microphone positions can vary for the impulse response and stationary signal measurements. In this work the data of the stationary signal is presented as a more reliable and clearer method of determining the spectral variation when a calibrated source is available.

The stationary levels are produced by a B&K 4296 omnidirectional source which emits pink noise and these levels are measured using MLSSA configured in Scope mode. The power level of emission is adjusted to 111 dB. The microphone used is the same as described before, thereby allowing calibration in situ.

III. CHURCHES ANALYZED

Twelve churches of the same typology varying in volume, dimensions, inner endings, and furnishing were acoustically reported. All these churches were built in the Middle Ages and their architectural style was a unique Spanish artistic movement since it was influenced by both Islamic and Christian Gothic elements.

The Mudejar-Gothic churches in Seville are morphologically characterized by this stylistic dualism: a vaulted Gothic apse and a body of three naves with a wooden timber roof (collar beam in the main nave) of Moorish origin. Its brick walls are complemented with portals and a stone apse. The supports are also clearly Islamic, with quadrangular or sometimes octagonal pillars and with raised brick moldings as decoration. Pointed, round, or segmental arches rest on these supports.

Among other elements of particular interest, funeral chapels have been added successively to the side naves and, on some occasions, are housed in remaining sections of pre-existing mosques. Funeral chapels do not exist in San Julián, San Esteban, and San Marcos churches.

According to the historian Angulo,¹⁴ the first Mudejar church built in Seville was Santa Marina; this church established the so-called *Seville parish type*. The 12 Catholic temples analyzed in this paper are all located in Seville's historical center.

Figure 1 shows the ground plan for each church under study with the source and receiver positions for measurements and the seating areas. These drawings are on the same scale and presented in order of decreasing volume. Table I summarizes some geometrical data of interest: volume V , length L , width W , average height H , total surface S_T , central nave ground surface S_C , lateral nave ground surface S_L , and total ground surface S_G , for the 12 churches. The congregational seating area consists of wooden pews with sometimes an additional group of seats and a textile carpet may be present at the entrance of the central nave. A complete description of the furnishings and other acoustic information on these temples has been published previously.¹⁵

IV. THEORETICAL MODELS

A. Introduction

The acoustic parameter prediction in churches is generally not an easy task. Simulation techniques may provide acceptable values of acoustic parameters but an elaborate three-dimensional model is an essential prerequisite. This complexity may discourage professionals from considering acoustic requirements for restoration or new designs.

Reverberation time is calculated through different well-known formulas. However, in religious buildings the calculation is more complicated since the different partial volumes

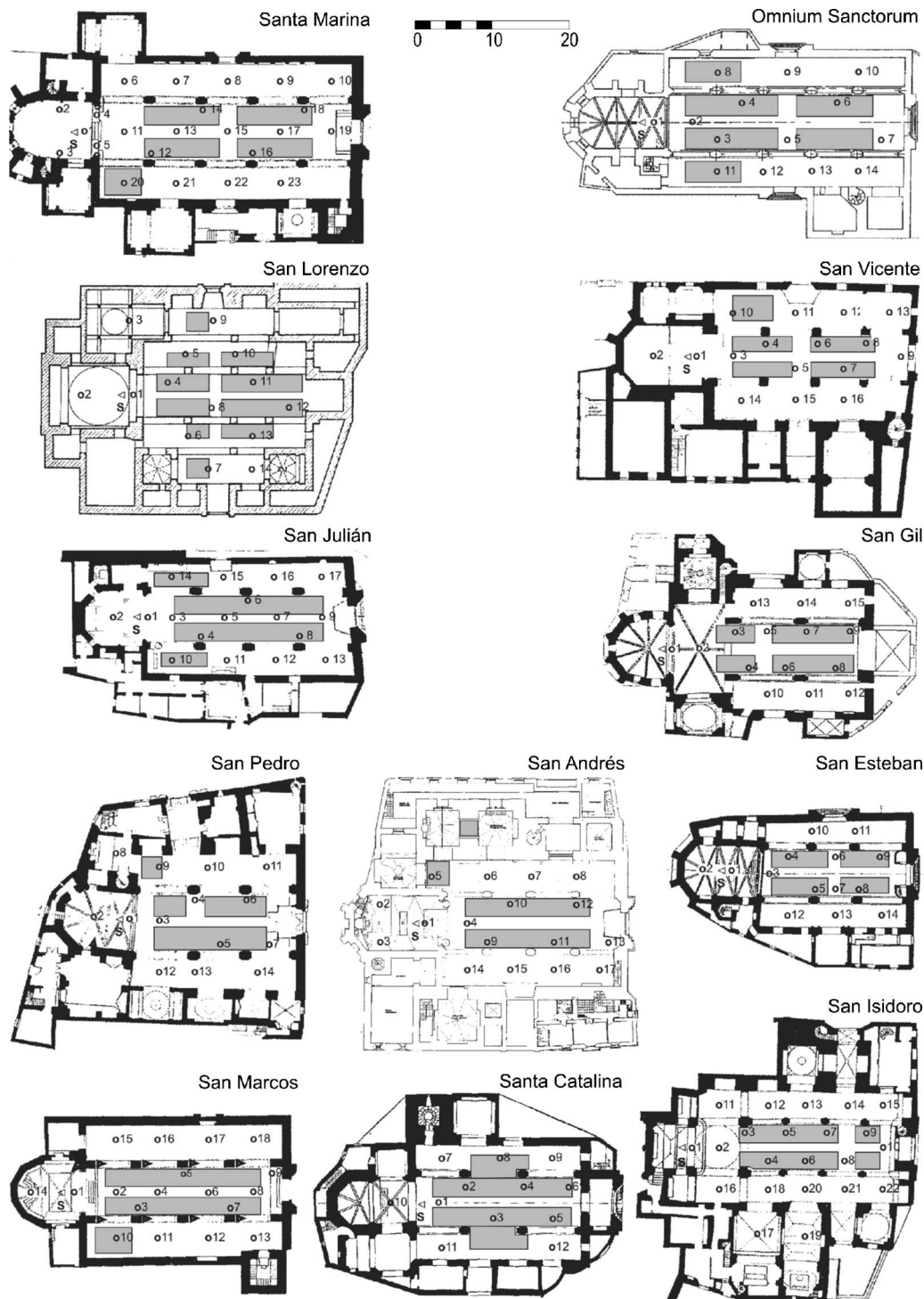


FIG. 1. Ground plan with the source (S) and receiver positions (o) for measurements and pew zone (shaded area) for the 12 churches (same scale for all churches).

which configure them, (chapels, vaults, lateral naves, choir seating, and other architectural elements), may be only partially coupled to the main volume and consequently the classic formulas do not properly account for the energy balance and reverberation times. Knudsen and Harris¹⁶ proposed a simple empirical method to adapt Sabine's equation to these enclosed rooms. In that work, an apparent absorption for the coupled surface in relation to the main volume is assigned. The effect of coupled spaces in churches has been well covered by Carvalho¹⁷ and Magrini and Ricciardi.¹⁸

If the geometry is not too complex, then the effect of coupling may be negligible in a first approximation or be dealt with by Carvalho's procedure, or by simplifications such as Kundsén's method, which allows reverberation times to be calculated. Predictions of other acoustic parameters are notably more difficult since they are more sensitive to position than reverberation time.

It has been verified^{19,20} that strong correlations between certain acoustic parameters exist, and that, even though they are statistically significant, there is no point in calculating

TABLE I. Geometrical data in Mudejar-Gothic churches.

Church	Reception	V (m ³)	L (m)	W (m)	H (m)	S_T (m ²)	S_C+S_L (m ²)	V/S_G (m ³ /m ²)
Sta. Marina	23	10,708	34	19	15	4517	250+279	20.24
O. Sanctorum	14	8180	29	16	16	3760	194+219	19.81
S. Lorenzo	14	7040	24	24	16	3346	132+267	17.64
S. Vicente	16	6915	26	18	11	3656	144+180	21.34
S. Julián	17	6226	27	15	13	3321	187+150	18.47
S. Gil	15	6200	22	15	14	3249	170+148	19.50
S. Pedro	14	6180	20	17	16	3035	123+154	22.05
S. Andrés	17	5955	23	15	11	3380	132+154	20.82
S. Esteban	14	4746	20	14.5	14	2691	141+134	17.26
S. Marcos	18	4623	26	17	10	3041	144+226	12.49
Sta. Catalina	12	4362	22	15	12	2474	121+102	19.56
S. Isidoro	22	3947	26	14.5	11	2547	133+144	14.25

some parameters as a function of others, since the last ones must be measured. Nevertheless, correlations between acoustic parameters and geometric characteristics, such as source-receiver distance, are useful and welcome. A theoretical model which implements these characteristics by accounting for the variation of the reflected acoustic field with source-receiver distance was proposed by Barron and Lee.⁷ This model has been widely used to predict G and C_{80} averaged values in concert halls and auditoria. However, it is not applicable in places of worship as has been highlighted by several authors.^{8,9,21} The reason is that in the presence of surfaces which are more diffusing in these spaces, the model tends to overestimate the early energy; the presence of certain architectural elements peculiar to churches, such as decorations and lateral chapels, affect the lateral energy in the first reflections as well, since sound is reflected according to complex paths which prevent them from returning to the main volume. Otherwise the disproportionate dimensions (length much greater than width and height) affect the sequence of arrival of reflected energy that follows immediately after direct sound.

B. Theoretical model revision

According to the ideal statistical theory of sound propagation in rooms, if the absorption is uniformly distributed and the sound field is diffuse, then the instantaneous normalized reflected energy density $\epsilon'(t')$, when taking the integrated energy density of the direct sound at 10 m E_{D10} as reference, is given by²²

$$\epsilon'(t') = \frac{\epsilon(t)}{E_{D10}} = \frac{13.82 \cdot 31,200}{V} e^{-\frac{13.82t'}{T}} (s^{-1}) \quad 0 \leq t' < \infty, \quad (2)$$

where $t'=0$ coincides with the emission of sound from the source, V is the volume, T the reverberation time and $\epsilon'(t')$ becomes dimensionless after integration. Implicit in this derivation is that the onset time of the reflected sound occurs simultaneously at all points through the space at the moment the direct sound is emitted.

All the acoustical parameters based on the energy may be calculated using Eq. (2), and will be expressed as a func-

tion of V , T , and r , the source-receiver distance. Direct sound (d) and total reflected energy (ℓ_T) are given by

$$d = \frac{100}{r^2}, \quad (3)$$

$$\ell_T = \int_0^\infty \epsilon'(\theta) d\theta = \frac{31,200T}{V}. \quad (4)$$

Hence the sound strength can be expressed as

$$\begin{aligned} G(r) &= L_P - L_{P_{10}} = 10 \log(d + \ell_T) \\ &= 10 \log\left(\frac{100}{r^2} + \frac{31,200T}{V}\right) (\text{dB}), \end{aligned} \quad (5)$$

where $G(r)$ in Eq. (5) is distance dependent due to the direct sound energy but not to the total reflected energy and hence, beyond the reverberant radius, the sound strength is uniform and takes the value $10 \log(31,200T/V)$ dB. The same happens with clarity, definition, and center time which tend towards $10 \log(e^{1.11/T} - 1)$ dB, $(1 - e^{-0.69/T})$ 100%, and $T/13.82$ s, respectively. However, measurement experimental data show this to be an oversimplification.

Barron and Lee⁷ developed a revised theory to take into account that reflected levels significantly decrease with increasing distance from the source in concert halls. The authors remarked that in those rooms the situation differed from diffuse requirements, mainly due to the concentration of absorption in the audience area. This model can be derived by reasoning that as reflected sound cannot arrive earlier than direct sound, the arrival of the direct sound can also be taken as the onset time of the reflected sound at that location. This can be explicitly expressed by writing $t' = t_D + t$ in Eq. (2), where $t_D = r/c$ is the flight time of direct sound from the source to the position at a distance r . Using this revised integration time gives a revised value for the instantaneous normalized reflected energy density which is now distance dependent:

$$\epsilon'_B(t,r) = \frac{\epsilon(t,r)}{E_{D10}} = \frac{13.82 \cdot 31,200}{V} e^{-\frac{0.04r}{T}} e^{-\frac{13.82t}{T}} (s^{-1})$$

$$0 \leq t < \infty, \quad (6)$$

where $t=0$ coincides with the arrival of direct sound at r distance. In other words, it supposes that, at location r , a pure exponential decay starts from the arrival of direct sound at that location and that reflected energy²³ is reduced at this point by a factor $e^{-\frac{0.04r}{T}}$ with respect to the classic expression of reflected sound energy.

In order to predict total sound pressure level and other indices, the sound energy is divided into three components: the direct sound (d) expressed in Eq. (3), the early reflected energy (e) (from 0 to τ ms), and the late reflected energy (ℓ) (from τ ms to infinity), with $\tau=80$ ms for clarity index and $\tau=50$ ms for definition index. The corresponding reflected energies in this model become:

$$e_B = \frac{31,200T}{V} e^{-\frac{0.04r}{T}} (1 - e^{-\frac{13.82\tau}{T}}), \quad (7)$$

$$\ell_B = \frac{31,200T}{V} e^{-\frac{0.04r}{T}} e^{-\frac{13.82\tau}{T}} \quad (8)$$

and consequently sound strength is given by

$$G_B(r) = 10 \log(d + e_B + \ell_B)$$

$$= 10 \log\left(\frac{100}{r^2} + \frac{31,200T}{V} e^{-\frac{0.04r}{T}}\right) \text{ (dB)}. \quad (9)$$

In the same manner, clarity and definition indices can be expressed as a function of source-receiver distance by

$$C_{80B}(r) = 10 \log\left(\frac{d + e_B}{\ell_B}\right)_{\tau=0.08}$$

$$= 10 \log\left(\frac{V e^{\frac{0.04r+1.11}{T}}}{312Tr^2} + e^{\frac{1.11}{T}} - 1\right) \text{ (dB)}, \quad (10)$$

$$D_{50B}(r) = \left(\frac{d + e_B}{d + e_B + \ell_B}\right)_{\tau=0.05}$$

$$\times 100 = \left(1 - \frac{\frac{31,200T}{V} e^{-\frac{0.04r+0.69}{T}}}{\frac{100}{r^2} + \frac{31,200T}{V} e^{-\frac{0.04r}{T}}}\right) \times 100 \text{ (\%)}. \quad (11)$$

Likewise center time becomes

$$T_{SB}(r) = \frac{\int_0^\infty t \epsilon'_B(t,r) dt}{d + e_B + \ell_B} = \frac{\frac{31,200T^2}{13.82V} e^{-\frac{0.04r}{T}}}{\frac{100}{r^2} + \frac{31,200T}{V} e^{-\frac{0.04r}{T}}} \text{ (s)}. \quad (12)$$

The aforementioned authors⁷ have verified the predictions of revised theory in many concert halls and auditoria mainly in order to establish G and C_{80} mean values.

In the same line, Vorländer²⁴ proposed for reverberant test rooms that the onset of reflected sound should start at the arrival of the first reflection and so, by substituting r in Barron's expression with the mean free path, the normalized reflected energy density is given by

$$\epsilon'_V(t) = \frac{\epsilon(t)}{E_{D10}} = \frac{13.82 \cdot 31,200}{V} e^{-\frac{A}{S}} e^{-\frac{13.82t}{T}} (s^{-1}), \quad (13)$$

where A is the absorption and S the surface of the enclosure.

Sendra, Zamarreño, and Navarro showed that reflected sound levels in Mudejar-Gothic churches generally fell below those predicted by Barron's revised theory. In their study, an adjustment parameter β , for each octave band, is experimentally determined through nonlinear regression in order to maximize correlation between predicted and measured sound level L_p data. Average values of β are proposed for general use in this specific type of church. According to their hypothesis, the normalized reflected energy density can be expressed for those spaces as

$$\epsilon'_\beta(t,r) = \frac{\epsilon(t,r)}{E_{D10}} = \frac{13.82 \cdot 31,200}{V} e^{-\frac{\beta r}{T}} e^{-\frac{13.82t}{T}} (s^{-1})$$

$$0 \leq t < \infty. \quad (14)$$

Again $t=0$ coincides with the arrival of direct sound at r distance. Equation (14) supposes that direct sound can be considered as the onset of reflected energy at location r , the same as in Barron's model, but the reflected energy is reduced by a factor $e^{-\frac{\beta r}{T}}$, where the β coefficient is determined experimentally as explained above. According to the paper by Sendra, Zamarreño, and Navarro,⁸ β coefficients oscillate between 0.06 and 0.12 (sm^{-1}) values which supposes larger factors of attenuations than in Barron's model. This loss of early energy is associated with the presence of certain architectural elements characteristic to churches, and therefore sound strength becomes

$$G_\beta(r) = 10 \log(d + e_\beta + \ell_\beta)$$

$$= 10 \log\left(\frac{100}{r^2} + \frac{31,200T}{V} e^{-\frac{\beta r}{T}}\right) \text{ (dB)}. \quad (15)$$

Equation (15) formally takes an expression similar to the corresponding Barron's Eq. (9). In fact, the expressions for the early and late reflected energies, clarity, definition and center time would be similar to the set of Eqs. (8)–(12), respectively, if 0.04 were replaced by β . Nevertheless, this model based on experimental G values failed to predict clarity and definition versus source-receiver distances in these churches as Galindo, Zamarreño, and Girón²⁵ pointed out. In their work they remarked that clarity and definition experimental values showed a larger decrease with respect to source-receiver distance than that obtained through the β model expected values, and that in fact the predictions from Barron's model and β adjustment coincided for those two indices. By means of the simple calculation below, those features can be shown explicitly. The differences between predicted Barron's values G_B and the β adjustment G_β for sound strength at great distances where direct sound can be negligible are given by

$$G_B - G_\beta \approx 10 \log\left(\frac{e_B + \ell_B}{e_\beta + \ell_\beta}\right) = 10 \log\left(e^{\frac{(\beta-0.04)r}{T}}\right) \\ = 4.3 \left(\frac{\beta-0.04}{T}\right)r. \quad (16)$$

Quantifying Eq. (16) for Santa Marina church for instance, $T=2.85$ s at the 2000 Hz band, $\beta=0.08$, at the rear part $r=35$ m, $G_B - G_\beta=2.1$ dB, which is a significant quantity. On the other hand, by taking into account clarity differences from the two models at the same source-receiver distance, a zero value is obtained:

$$C_{80B} - C_{80\beta} \approx 10 \log\left(\frac{e_B \times \ell_\beta}{e_\beta \times \ell_B}\right) = 10 \log(1) = 0. \quad (17)$$

The same conclusion can be reached for the definition index. As both the revised theory and the β model introduce attenuations of the reflected energy which affects early and late energy equally, they are unable to predict energy indices based on early-to-late or early-to-total ratios.

A more general model to be applied to rooms with asymmetrical absorption was proposed by Arau.²⁶ The model is based in revised theory but the author divided the extinction decay curve into three different parts with different slopes, the initial early sound, the early sound, and the late sound, respectively. The rhythm of the two first is governed by the early decay time (EDT) and by the mean reverberation time. The principal disadvantages of this model are its complexity and the fact that it is largely based on EDT values which are very sensitive to location and hence difficult to predict.

Recently Cirillo and Martellota⁹ derived a modified theory and an alternative adjustment to the energy density for a type of church. Their solution assumes that the linear level decay starts after a certain delay time t_R after the arrival of the direct sound, which is considered $t=0$ in this work, and which is proportional to the source-receiver distance, $t_R = \rho r$. The constant of proportionality ρ is determined experimentally by establishing a similitude of churches according to room characteristics. They derived a correction on this basis and accounted for the specific early reflection pattern as proposed by Vorländer²⁴ such that the instantaneous normalized energy density can be written as

$$\epsilon'_C(t, r) \\ = \frac{\epsilon(t, r)}{E_{D10}} \\ = \begin{cases} \left(\frac{\epsilon'_B(t_R) - \gamma d}{t_R}\right)t + \gamma d \text{ (s}^{-1}\text{)} & 0 \leq t \leq t_R, \\ \frac{13.82 \cdot 31,200}{V} e^{-\frac{(0.04+13.82\rho)r}{T}} e^{-\frac{13.82t}{T}} \text{ (s}^{-1}\text{)} & t_R \leq t < \infty, \end{cases} \quad (18)$$

where the factor γ weights the magnitude of the early reflections against the direct sound d and depends on the mean absorption coefficient, the mean scattering coefficient, and the mean free path of the church. Although the model was initially tested for Apulian Romanesque churches,⁹ ulti-

mately they have refined it to provide a more reliable and physically acceptable hypothesis and have extended their prediction to other types of churches.¹⁰ They have established some sort of typological behavior and the comparison of their predictions with the experimental values for sound strength, clarity, and center time is reasonably accurate. However, the model does not retain the simplicity in the calculations of the other statistical formulas.

C. Proposed model

Gade²⁷ carried out a statistical analysis of room acoustical and architectural data from 32 concert halls in order to look for relationships between spatially averaged acoustic parameters and various design variables. The author reached the conclusion that volume and reverberation time are the main factors governing the behavior of the acoustic parameters which measure level, reverberance, and clarity. However, geometrical factors have an additional influence on clarity and, particularly on spaciousness and on the conditions for musicians on the orchestra platform. This author suggests that the results point towards the possibility of obtaining empirical formulas by means of regression that would predict the values of the acoustic parameters in halls, if their reverberation time and geometry were known.

In this context, following Gade's ideas and taking advantage of the relevant contribution by Barron, it would be interesting to model the observed additional attenuation in the acoustic energy parameters as a function of source-receiver distance. The proposed model tries to retain the simplicity of Barron's revised theory and tune it according to experimental data. In this way it will be possible to implement typological models in terms of architectural characteristics that could be applied in an immediate way to make design decisions.

With the purpose of comparing the extinction curves at different distances in these spaces, these curves have been superimposed at the 1000 Hz octave band for two churches studied, that of the largest volume and one of the most reverberant Santa Marina church, and another smaller and less reverberant Santa Catalina church. In Fig. 2(a) the decay trace for different reception points belonging to Santa Marina central nave and Fig. 2(b) for different reception points belonging to its lateral nave are shown. Likewise, Figs. 2(c) and 2(d) show the equivalent results for Santa Catalina church. In each case the curve corresponding to the nearest point in front of the source located on the central nave has been chosen as a reference, and hence vertical scale is relative. However, the temporary axis is absolute and has its origin at the instant the source starts emitting.

Although all curves decay linearly and with the same attenuation rhythm, remarkable differences appear in the initial parts for both churches. On trying to model this behavior with the mentioned β adjustment model proposed by Sendra Eqs. (14) and (15), the early and late energies are reduced by the same attenuation factor which is adjusted through non-linear regression from the measured global levels. However, trying to predict the behavior of the energy parameters with this method, produced values which were very near those derived from Barron's pattern and far from experimental data

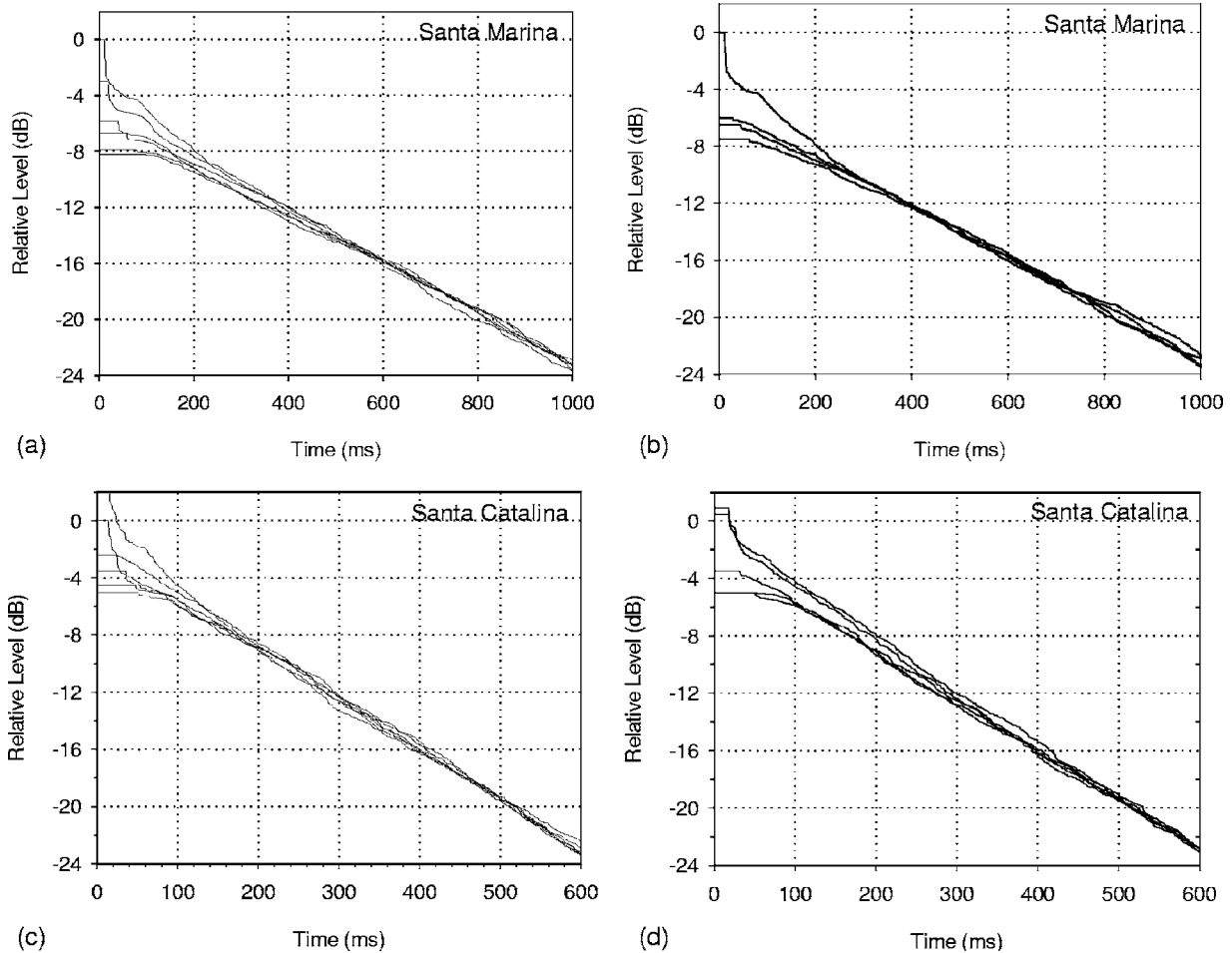


FIG. 2. Extinction decay traces at several location points at the 1000 Hz band in Santa Marina church, (a) central nave, (b) lateral nave; and in Santa Catalina church (c) central nave, (d) lateral nave. In this graph, time $t=0$ coincides with the time of emission of the source, and the vertical scale is relative: 0 dB corresponds to the stationary level of the nearest point to the source in the central nave.

as has already been mentioned. Other approaches need to be considered that, without losing the simplicity of the pattern, allow the prediction of the values of all energy parameters appropriately.

To reach this objective, the first part of the energy-time curves measured in churches has been analyzed. In Figs. 3(a)–3(d), these curves appear octave filtered at 1 kHz, for positions 11, 13, 15, and 17 respectively, located in the central nave of Santa Marina church (see Fig. 1). In each case, the first cursor (dotted vertical line) shows the arrival time of the direct sound and the second cursor (continuous vertical line) is placed 80 ms later. This is the usual time limit interval to calculate early and late energy indices. It can be observed how the pattern of first reflections shows complex behavior that can also be observed by ray-tracing simulation using Catt Acoustic (see Fig. 4, which shows complete and early simulated echograms for position 15 in Santa Marina church).

In order to retain the simplicity of the model, this behavior can be modeled by considering a linear level attenuation with the same rate as the classic theory for early energy and by assuming an additional attenuation. This supposes a discontinuity at $t=80$ ms that will be discussed in the next

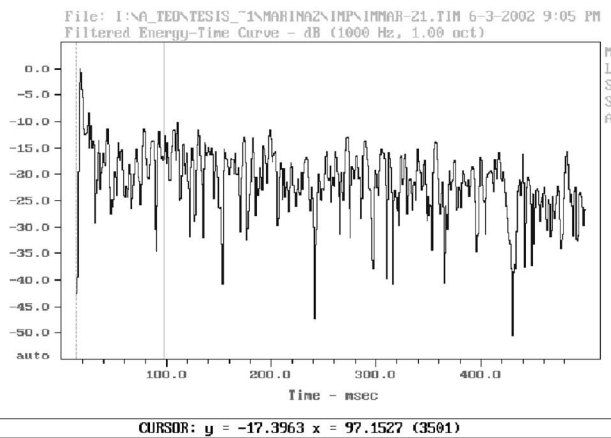
section and is shown qualitatively in Fig. 3(d) by means of the superimposed straight lines.

The best option for the evaluation of this additional attenuation appears by adjusting the early energy expression such as is written in Eq. (19) (considering $\tau=0.08$ s)

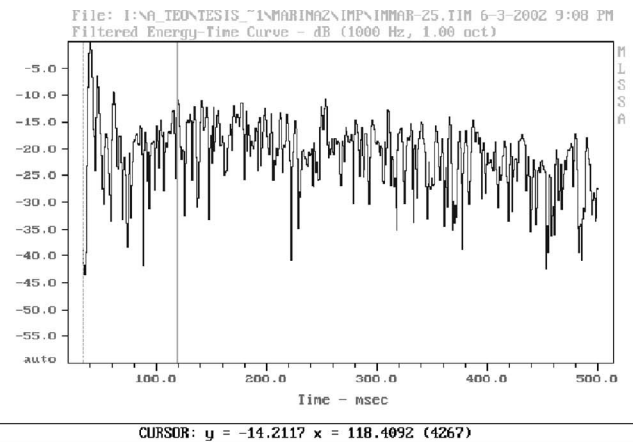
$$e_{\mu} = \frac{31,200T}{V} e^{-\frac{\mu r}{T}} (1 - e^{-\frac{13.82\tau}{T}}) \quad (19)$$

to the spatial distribution of the experimental values of C_{80} instead of those of G as in Sendra, Zamarreño, and Navarro,⁸ and by supposing that the late energy behaves in the same way as in Barron's model $\ell_{\mu}=\ell_B$; with $\tau=0.08$, Eq. (8). Henceforth this will be known as the μ model.¹¹

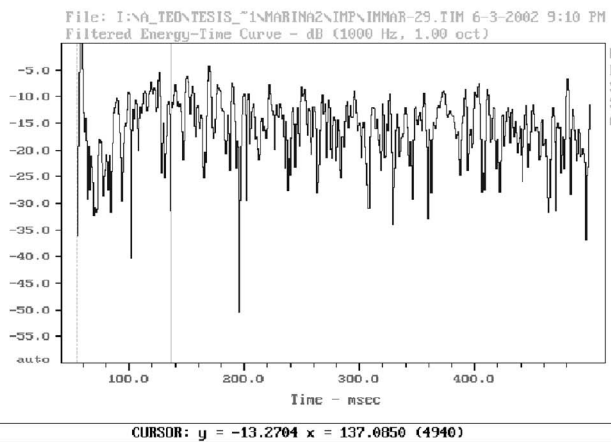
An evaluation has been carried out of the differences in the total energy, or in other words of $G_{\mu}(r)$, by considering $\tau=50$ ms and $\tau=80$ ms limits as the temporal interval to separate early and late energy. As a function of distance in Fig. 5(a), early, late, and total temporal energy values for Santa Marina church are shown, taking $\tau=50$ ms and $\tau=80$ ms as separation limits in Eqs. (19) and (8), respec-



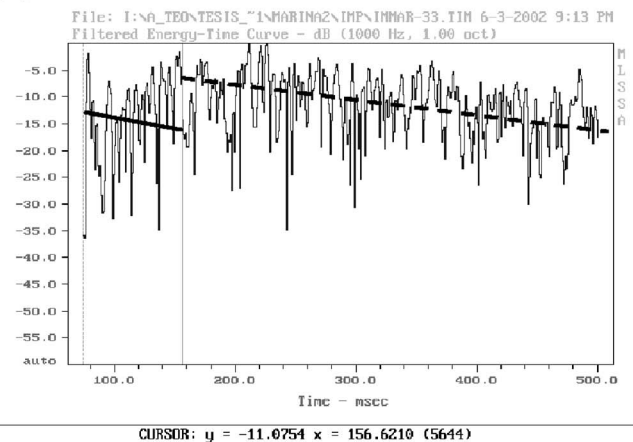
(a)



(b)



(c)



(d)

FIG. 3. Energy-time curves measured in Santa Marina church at positions 11 (a), 13 (b), 15 (c) and 17 (d) in the central nave. The 80 ms interval after the arrival of direct sound is located between vertical cursors. In (d) the qualitative behavior of the proposed model is superimposed.

tively. $G_{\mu}(r)$ differences (Fig. 5(b)), when choosing one or the other separation limit, are in the order of 0.4 dB at the farthest measurement points of this church, approaching the experimental values better, those of $G_{\mu 80}(r)$. In consequence, the $\tau=80$ ms limit following Barron's criterion has been used in the following sections.

The values of μ coefficient, for each church, obtained through nonlinear regression process in order to maximize the correlation between predicted and experimental values of C_{80} , are shown in Table II. As before, their volumes V and

measured reverberation times T are exposed as the whole set of data required to implement this model, and in the last two lines the mean value $\bar{\mu}$ and its standard deviation σ_{μ} appear. This mean value can be used to describe the behavior of this specific church typology in order to estimate any parameter. On proposing this $\bar{\mu}$ mean value it is verified that the set of values (except San Julián church) are included in the $\bar{\mu} \pm 1.5\sigma_{\mu}$ interval.

The expression of clarity $C_{80\mu}$ (remembering this is the parameter that has been used in the regression) becomes

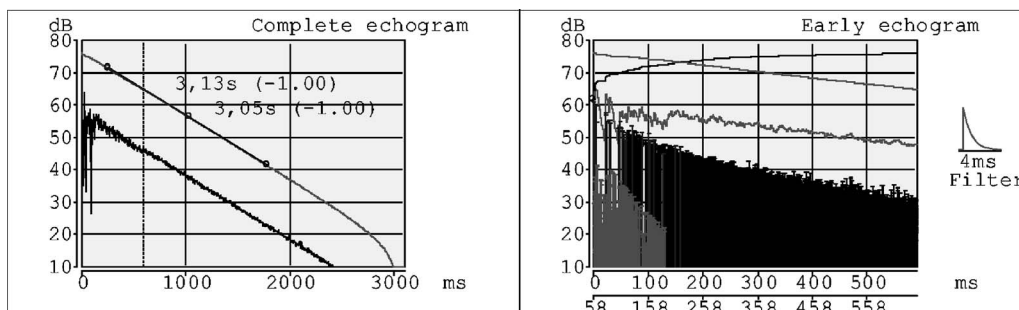


FIG. 4. Simulated echograms in Santa Marina church at position 15 in the central nave.

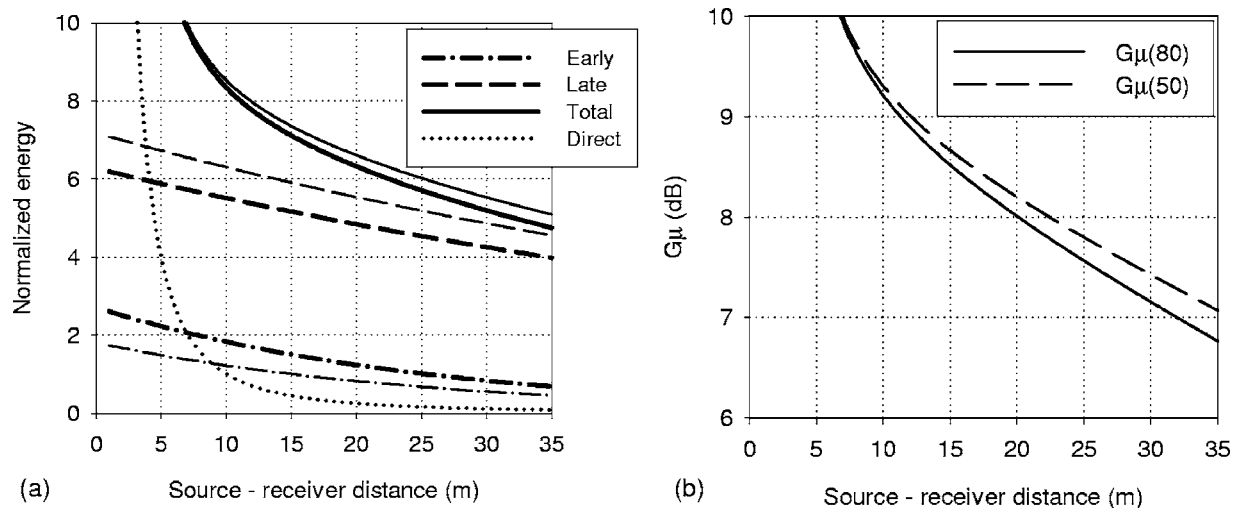


FIG. 5. Theoretical behavior of, (a) normalized energy components (fine line for $\tau=50$ ms), (heavy line for $\tau=80$ ms) and (b) their corresponding G_μ vs source-receiver distance in the proposed model, for Santa Marina church.

$$C_{80\mu}(r) = 10 \log \left(\frac{d + e_\mu}{\ell_B} \right)_{\tau=0.08}$$

$$= 10 \log \left\{ \frac{\frac{100}{r^2} + \frac{31,200T}{V} e^{-\frac{\mu r}{T}} (1 - e^{-\frac{1.11}{T}})}{\frac{31,200T}{V} e^{-\frac{1.11+0.04r}{T}}} \right\} \text{ (dB)}. \quad (20)$$

The definition will be expressed in a similar way, bearing in mind that the separation limit is now $\tau=50$ ms for e_μ in its nominator and, $\tau=80$ ms for e_μ in its denominator:

$$D_{50\mu}(r) = \frac{(d + e_\mu)_{\tau=0.05}}{(d + e_\mu + \ell_B)_{\tau=0.08}} \times 100$$

$$= \left\{ \frac{\frac{100}{r^2} + \frac{31,200T}{V} e^{-\frac{\mu r}{T}} (1 - e^{-\frac{0.69}{T}})}{\frac{100}{r^2} + \frac{31,200T}{V} [e^{-\frac{\mu r}{T}} (1 - e^{-\frac{1.11}{T}}) + e^{-\frac{1.11+0.04r}{T}}]} \right\} \times 100 \text{ (\%)}. \quad (21)$$

TABLE II. Input parameters to implement the proposed model

Church	V (m ³)	T (s)	μ (s/m)
Sta. Marina	10,708	3.08	0.1210
O. Sanctorum	8180	2.71	0.1400
S. Lorenzo	7040	2.28	0.1392
S. Vicente	6915	2.47	0.1571
S. Julián	6226	2.27	0.0901
S.Gil	6200	2.27	0.1200
S. Pedro	6180	2.04	0.1303
S. Andrés	5955	1.99	0.1520
S. Esteban	4746	1.87	0.1277
S. Marcos	4623	3.58	0.1604
Sta. Catalina	4362	1.60	0.1072
S. Isidoro	3947	2.21	0.1324
		Mean value $\bar{\mu}$	0.1314
		Standard deviation σ_μ	0.0205

After substituting d , e_μ , and ℓ_μ with $\tau=80$ ms in Eqs. (20) and (21), sound strength is written as

$$G_\mu(r) = 10 \log(d + e_\mu + \ell_B)$$

$$= 10 \log \left\{ \frac{100}{r^2} + \frac{31,200T}{V} \times [e^{-\frac{\mu r}{T}} + e^{-\frac{1.11}{T}} (e^{-\frac{0.04r}{T}} - e^{-\frac{\mu r}{T}})] \right\} \text{ (dB)}, \quad (22)$$

which in the case $\mu=0.04$ sm⁻¹, Eq. (22) would coincide with Barron's proposal and so corresponds to the whole model. As shown in Table II, μ values are significantly larger than 0.04 in all these Mudejar-Gothic churches.

Only partial C_{80} estimated values (for 1 kHz octave band) versus source-receiver distances are available from some papers for different churches.^{9,10} From these values their corresponding μ coefficients have been estimated. These corresponding attenuation factors μ for the early energy are volume dependent (Fig. 6(a)). This dependence increases when μ is plotted on a graph versus the geometric ratio V/L , as Fig. 6(b) shows. The V/L ratio can be taken as a measure of the area of transversal section and so the higher the values of V/L are, the more attenuation for early energy is expected. Some acoustic characteristics have an additional incidence over the attenuation of the early energy: the presence of scattering surfaces such as altarpieces, altars and pillars, and the timber roof characteristic to these Mudejar-Gothic churches; in this case lateral naves and chapels act as coupled rooms which diminish the reflected energy from the laterals to the main volume. Although more precise measurements are required, it is possible to establish that the μ value for each Mudejar-Gothic church can be substituted by their mean value in order to characterize this ecclesiastical typology. Deeper analyses into this topic are accomplished in Sec. V.

An expression for the instantaneous normalized reflected energy density $e'(t, r)$, deducible from e_μ and $\ell_\mu = \ell_B$, Eqs. (19) and (8), respectively, would be

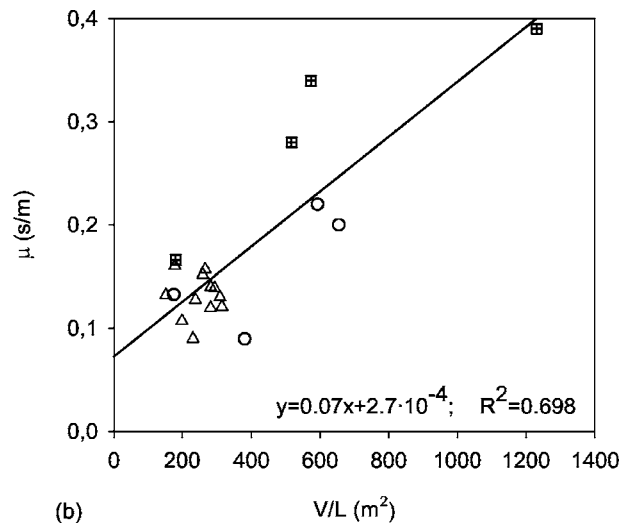
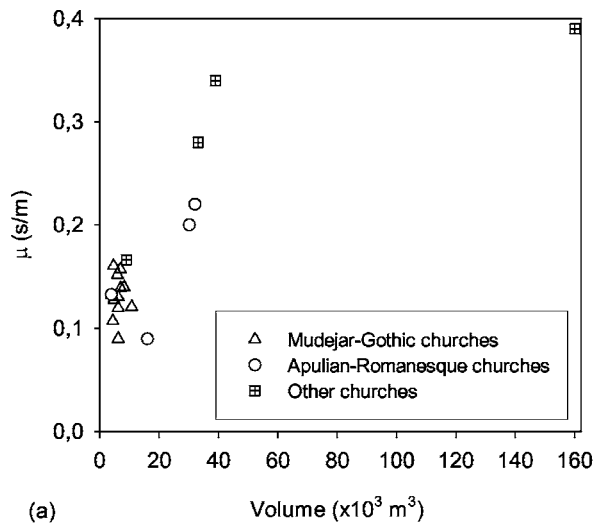


FIG. 6. Values of μ for Mudejar-Gothic and other churches vs volume (a) and vs volume-length ratio (b).

$$\begin{aligned} \epsilon'_\mu(t,r) &= \frac{\epsilon(t,r)}{E_{D10}} \\ &= \begin{cases} \frac{13.82 \cdot 31,200}{V} e^{-\frac{\mu T}{T}} e^{-\frac{13.82t}{T}} (s^{-1}) & 0 \leq t \leq 80 \text{ ms}, \\ \frac{13.82 \cdot 31,200}{V} e^{-\frac{0.04r}{T}} e^{-\frac{13.82t}{T}} (s^{-1}) & 80 \text{ ms} < t < \infty, \end{cases} \end{aligned} \quad (23)$$

where $t=0$ coincides in this expression with the arrival of direct sound at r location. This reflected energy proposal supposes that the decay traces can be modeled in two steps: the first beginning at the arrival of direct sound at that location where stationary reflected energy is reduced by a factor $e^{-\frac{\mu r}{T}}$ with respect to the classic expression, which is distance dependent and finishes at 80 ms; the second step from 80 ms on corresponds to that decay considered in Barron's hypothesis. Figure 7 shows the magnitude of the step at 80 ms, as a function of source-receiver distance for Santa Marina and Santa Catalina churches. Santa Catalina

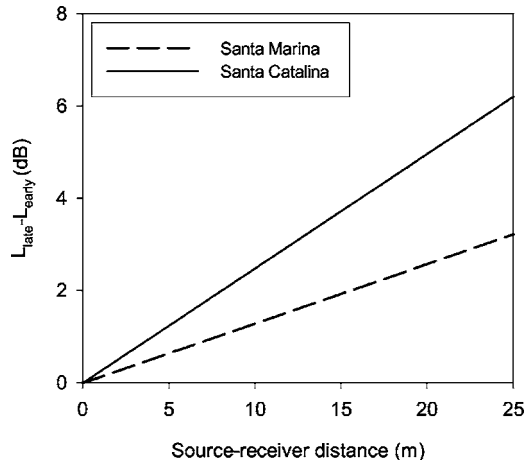


FIG. 7. Differences between early and late energies at $t=80$ ms for the μ model as a function of source-receiver distance for two significant churches.

church is the most profusely decorated, and in this way increases the scattering properties of its surfaces and shows major attenuations for all distances.

In this way center time can be deduced by means of

$$T_{S\mu}(r) = \frac{\int_0^{0.08} t\epsilon'_\mu(t,r)dt + \int_{0.08}^{\infty} t\epsilon'_\mu(t,r)dt}{d + e_\mu + \ell_B} (s), \quad (24)$$

which, according to Eq. (23), becomes an immediate integral. Although this proposed normalized reflected energy density presents a discontinuity at 80 ms, it should be observed that the extinction process is physically discrete and hence this approximation to reality cannot be considered as inadequate at all, particularly when taking into account the very good agreement between the experimental results and the theoretical values for center time (see Figs. 8(d) and 11(d), and Tables III and IV), whose calculations have been carried out with this proposed discontinued normalized reflected energy density.

V. DISCUSSION OF THE MODEL

The procedure established here has been applied to the set of churches under study in order to check its reliability. Figure 8 shows the predictions with this μ adjustment and the experimental values for the four energy-based parameters analyzed: clarity, definition, sound strength, and center time versus source-receiver distance in Santa Marina church.¹¹ Likewise, Figs. 9–11 show the same theoretical predictions and the experimental results for San Julián, San Esteban, and Santa Catalina churches, respectively. Every single graph shows a significant deviation from Barron's predictions in all parameters studied which has been taken as a reference model that is able to predict the attenuations of early-to-late energy parameters with source-receiver distances.

Both models are based on modeling first reflections before direct sound reaches the reception position. In this sense, the sequence and magnitude of early reflections are

TABLE III. Differences between measured values, calculated values according to Barron's model, and the proposed model which have been spatially averaged for the four energy-based parameters.

Church	C_{80} (dB)		D_{50} (%)		G (dB)		T_s (ms)	
	Barron	Proposed	Barron	Proposed	Barron	Proposed	Barron	Proposed
Sta. Marina	2.7	0.6	6.7	0.1	0.8	0.1	46	-14
O. Sanctorum	2.1	-0.5	6.8	-2.0	1.3	0.5	37	2
S. Lorenzo	2.4	0.0	7.5	-1.5	1.4	0.5	32	3
S. Vicente	2.6	-0.4	9.9	-0.6	1.2	0.3	42	2
S. Julián	1.9	0.3	3.7	-1.9	1.5	0.7	18	6
S. Gil	2.1	-0.3	4.6	-4.2	2.1	1.2	28	8
S. Pedro	1.9	-0.3	7.7	-1.2	0.0	-0.9	22	11
S. Andrés	3.4	0.3	12.6	0.6	-0.1	-1.2	35	9
S. Esteban	2.4	-0.5	9.8	-1.5	0.9	-0.5	27	14
S. Marcos	3.0	0.2	7.4	0.5	1.5	0.7	37	-1
Sta. Catalina	1.2	-0.6	6.1	-2.2	0.7	-0.2	14	14
S. Isidoro	2.6	-0.2	10.7	0.1	2.0	0.9	39	3
Average	2.4	-0.1	7.8	-1.2	1.1	0.2	31	5

strongly influenced by the geometric and acoustic characteristics near the source and near the different reception positions, especially the scattering properties of these surfaces as has been suggested by Chiles²³ and Cirillo.¹⁰

In this case, the source position is in the main altar where the usual presence of elaborately decorated altarpieces and furniture produce scattered reflected energy near the source which is seldom found in concert halls. In a similar

way, near each receiver position we can find pillars, lateral altars and chapels, wooden pews, a diffusing timber roof (the main characteristic of these churches), which all have a scattering effect on the early reflected energy. In this manner the patterns of first reflections are different in churches to other buildings. In order to retain the simplicity of Barron's model, additional attenuation has been considered for the early reflected energy as shown in Eq. (19). It has also been checked

TABLE IV. Mean values of the absolute value differences between those calculated from Barron's model and from the proposed model and the measured values in each position (first row), and their corresponding standard deviation (second row) for each church.

Church	C_{80} (dB)		D_{50} (%)		G (dB)		T_s (ms)	
	Barron	Proposed	Barron	Proposed	Barron	Proposed	Barron	Proposed
Sta. Marina	1.4	0.9	7.6	3.6	0.9	0.4	47	20
	0.9	0.8	3.8	3.4	0.5	0.3	24	12
O. Sanctorum	2.2	1.2	9.4	5.3	1.5	0.9	40	20
	1.9	1.0	5.5	4.9	0.9	0.7	30	14
S. Lorenzo	2.4	0.5	8.8	3.1	2.0	1.2	35	10
	1.3	0.3	4.6	2.9	0.8	0.8	16	8
S. Vicente	2.8	1.2	11.7	4.5	1.4	0.7	46	16
	1.0	0.9	3.1	4.6	0.5	0.6	13	13
S. Julián	2.2	1.2	9.4	6.1	1.5	0.7	26	12
	1.5	0.6	5.7	6.0	0.6	0.4	14	11
S. Gil	2.2	0.9	7.3	5.3	2.2	1.5	32	14
	1.5	0.6	4.3	4.8	1.1	0.6	21	10
S. Pedro	2.3	1.5	11.7	8.5	0.6	0.9	32	21
	1.3	1.5	6.3	8.4	0.6	0.8	15	27
S. Andrés	3.4	1.8	12.6	6.4	0.6	1.3	35	24
	2.6	1.8	8.5	5.0	0.5	0.6	24	11
S. Esteban	2.5	0.7	10.2	3.3	1.3	0.8	30	14
	1.2	0.4	6.2	2.2	0.7	0.7	15	9
S. Marcos	3.2	1.4	7.6	3.3	1.7	1.0	44	25
	1.5	0.9	4.0	1.9	0.6	0.6	23	15
Sta. Catalina	2.4	1.2	13.9	7.4	1.5	1.0	28	15
	1.1	1.1	4.9	6.6	0.7	0.7	12	13
S. Isidoro	2.7	0.7	10.9	3.7	2.2	1.3	41	13
	1.5	0.6	5.8	2.3	1.0	0.6	24	12
Average	2.5	1.1	10.1	5.0	1.5	1.0	36	17
	1.4	0.9	5.2	4.4	0.7	0.6	19	13

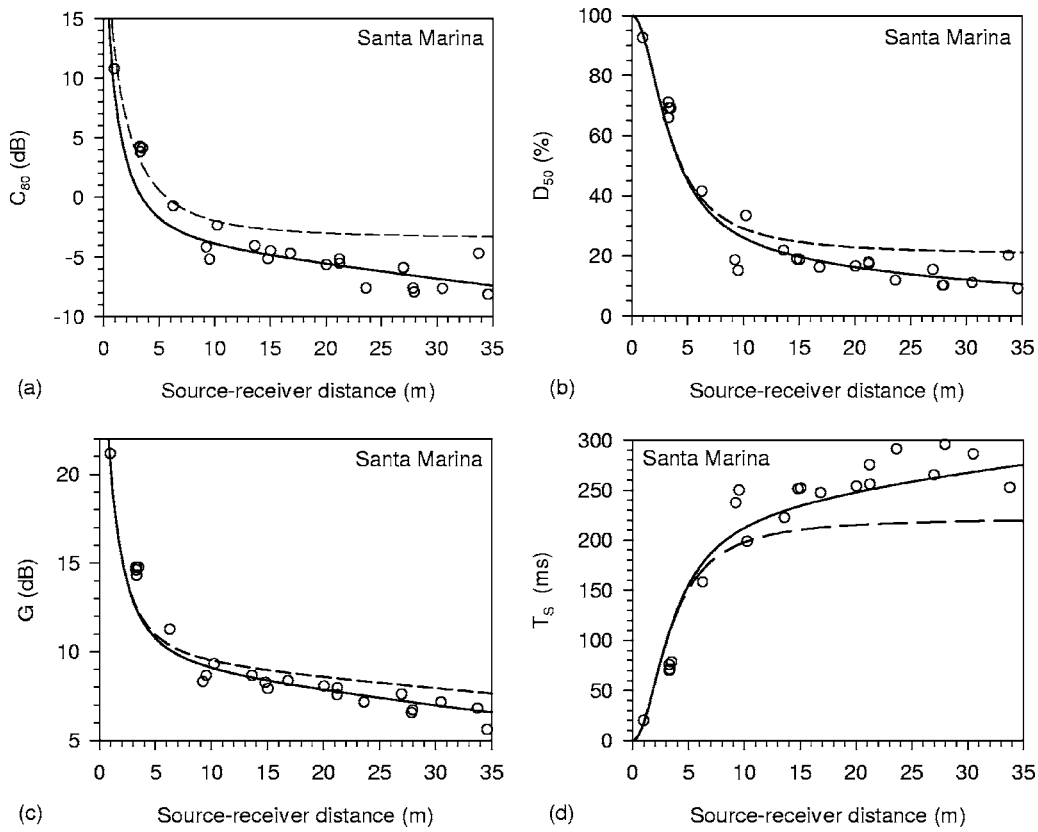


FIG. 8. Santa Marina church, measured values (o) and calculated values from Barron's model (dashed line) and from the proposed model (continuous line), vs source-receiver distance: (a) C_{80} , used to obtain μ through nonlinear regression, (b) D_{50} , (c) G , and (d) T_s .

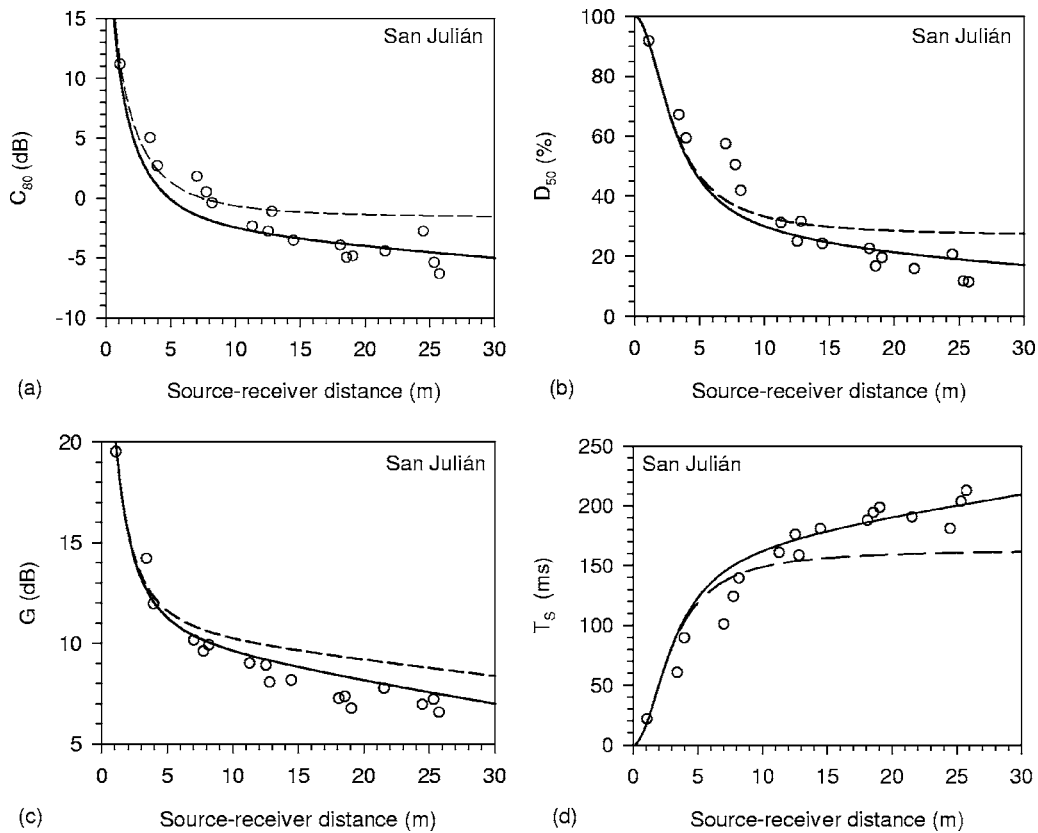


FIG. 9. San Julián church, measured values (o) and calculated values from Barron's model (dashed line) and from the proposed model (continuous line), vs source-receiver distance: (a) C_{80} , used to obtain μ through nonlinear regression, (b) D_{50} , (c) G , and (d) T_s .

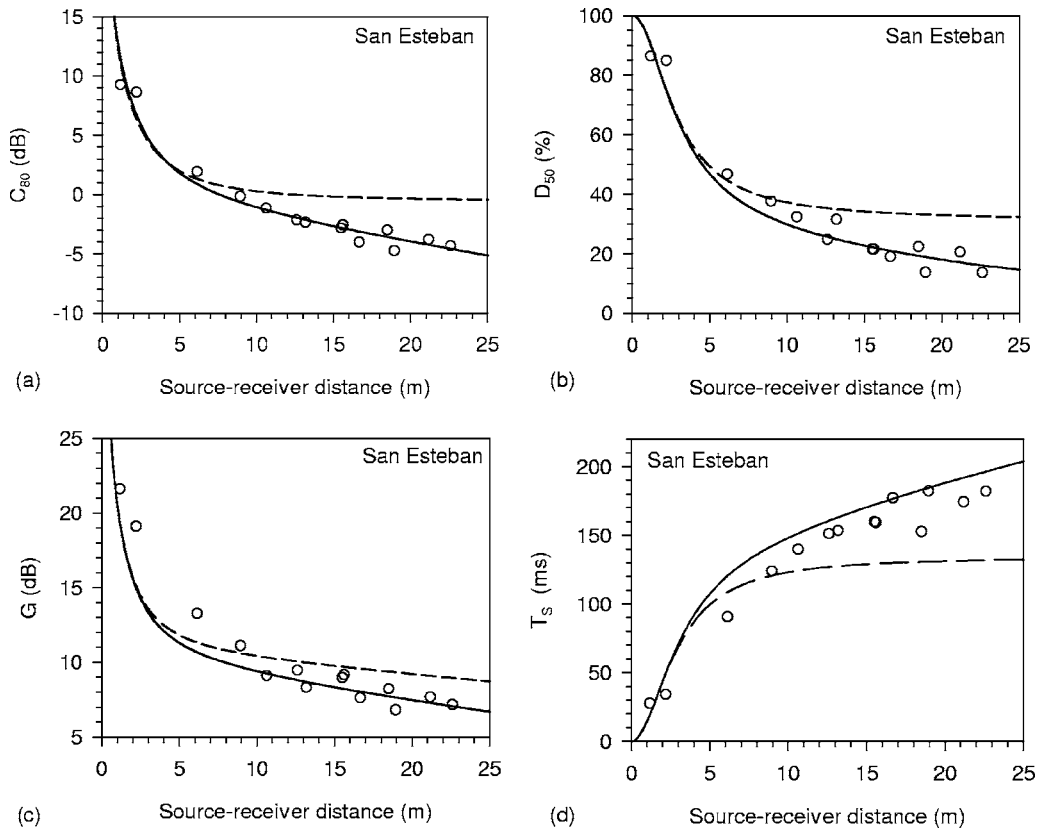


FIG. 10. San Esteban church, measured values (o) and calculated values from Barron's model (dashed line) and from the proposed model (continuous line), vs source-receiver distance: (a) C_{80} , used to obtain μ through nonlinear regression, (b) D_{50} , (c) G , and (d) T_s .

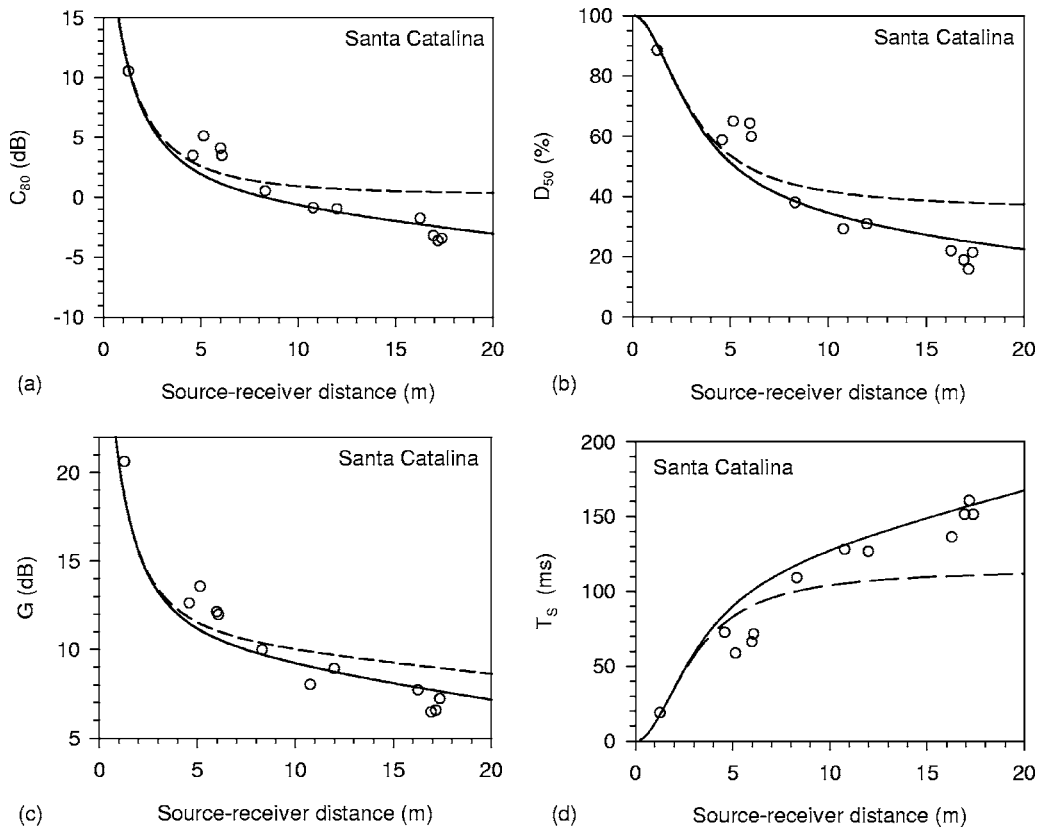


FIG. 11. Santa Catalina church measured values (o) and calculated values from Barron's model (dashed line) and from the proposed model (continuous line), vs source-receiver distance: (a) C_{80} , used to obtain μ through nonlinear regression, (b) D_{50} , (c) G , and (d) T_s .

in some cases that, in accordance with Carvalho's¹⁷ paper, the apse (where the source is located) behaves as a coupled space.

From the set of Figs. 8–11, it may be highlighted that, due to the coupling effect, there are differences between predictions and measurements in points belonging to the presbyteries at short distances from the source. In the farthest points belonging to the lateral naves some discrepancies also exist due to the scattering effect near the reception positions.

The results of the calculation both through the proposed model and Barron's model have been compared with the measured data in each church. Table III shows the differences between measured and calculated values according to Barron's model and the proposed model which have been spatially averaged for the four energy-based parameters. Since C_{80} values have been used to obtain the μ coefficients and thereby the proposed model is tuned to experimental data, the differences between measured and calculated spatially averaged values are slight for the proposed model. This observation is taken into account below and hence Barron's model is considered as a reference and not as a comparison. Clarity values vary from 3.4 dB for San Andrés church to 1.2 dB for Santa Catalina church in Barron's model (average, differences of 2.4 dB for the set of churches). For the proposed model this interval is reduced to 0.6 dB for Santa Marina church to -0.6 dB for Santa Catalina church with average differences of -0.1 dB for all churches. Obviously Barron's model tends to overestimate C_{80} values.

The differences between measured and calculated spatially averaged values for D_{50} oscillates from 12.6% for San Andrés church to 3.7% for San Julián church in Barron's model and between 0.6% for San Andrés church and -4.2% for San Gil church in the proposed model. For all churches the averages of these differences are 7.8% for Barron's model and -1.2% for the proposed model. In this case Barron's model also overestimates D_{50} values, whereas the proposed model fluctuates between overestimating in some cases and underestimating in others.

For G parameter the range of variation oscillates between 2.1 dB for San Gil church and -0.1 dB for San Andrés church with an average value for all churches of 1.1 dB for Barron's model, whereas for the proposed model the oscillation is between 1.2 dB for San Gil church and -1.2 dB for San Andrés church and an average value of 0.2 dB. Although in this parameter Barron's model may suppose a better approach in some churches (San Andrés) average values lean clearly towards the proposed model.

The improvement in prediction for T_S values is remarkable in favor of the proposed model. The differences from spatially averaged values from Barron's model vary between 46 ms for Santa Marina church and 14 ms for Santa Catalina church. In the proposed model this interval is reduced to 14 ms for Santa Catalina church and -14 ms for Santa Marina church with an average difference of 31 ms for Barron's model against 5 ms in the proposed model.

Continuing with this analysis, Table IV shows the average absolute values (first row for each church), and their respective standard deviation (second row for each church) of the differences between predicted parameter values and

measured ones for each position. In this way it is possible to assess the improvement that the proposed model supposes on predicting the variation of the different parameters with the source-receiver distance. For these temples mean values of those differences in C_{80} are significantly lower in the proposed model, as can be seen in Table IV. Moreover, its dispersions are notably lower (except San Pedro church). For the whole set of churches, mean value of the differences diminishes from 2.5 dB obtained in Barron's model to 1.1 dB in the proposed model and the mean value of the standard deviation is reduced from 1.4 to 0.9 dB.

Something similar happens for the D_{50} parameter: in each church average differences are significantly lower in the proposed model than in Barron's model, and in the whole set mean value is reduced from 10.1% for Barron's model to 5.0% in the new proposal. Dispersions of these differences from the mean value in each church are higher in the proposed model in four churches: San Vicente, San Gil, San Pedro, and Santa Catalina. For the set as a whole, the mean value of the dispersions decreases from 5.2% for Barron's case to 4.4% in the proposed model.

The same comments can be applied to the prediction of the proposed model in the spatial distribution of G values for all churches, except San Pedro and San Andrés. For this parameter, the accuracy of the model proposed is less notable due to the lower relative weight of the early energy. The differences in the dispersions described by standard deviation are similar in both models. For the whole set of churches the average of the differences moves from 1.5 dB (Barron), to 1.0 dB (proposed model). The average value of standard deviation is similar (0.7 and 0.6 dB, respectively).

Finally, it should be mentioned that the greatest improvement appears in the T_S values. The differences are reduced by half in each church for all churches and the average difference is reduced from 36 ms (Barron) to 17 ms (proposed model). The standard deviation is also reduced from 19 to 13 ms.

Table III and Table IV data confirm that a considerable improvement is provided by the proposed model for this kind of space as compared with Barron's revised theory, in clarity, definition, and center time and a more modest improvement for G .

The analysis is extended in Figs. 12(a) and 12(b) by means of a comparison between the different temporal energy components calculated through: Barron's model (B); Cirrillo's model (C), estimating from their suggestions¹⁰ a $\rho=0.0058$ sm^{-1} value and a dispersion coefficient $s=0.20$; and the proposed model (P); all versus source-receiver distance for both Santa Marina and San Marcos churches. In these figures, the direct sound, which is common to the three models, their respective early reflected energy (received until 80 ms after the arrival of direct sound), their late reflected energy (from 80 ms to infinity), and total energy, respectively, are shown.

Several aspects of the graphs should be emphasized. In the early reflected energy, Barron's values present a great deviation from the two other models; on comparing Cirrillo's and the proposed μ adjustment, the former gives greater values in the vicinities of the source and greater attenuations at

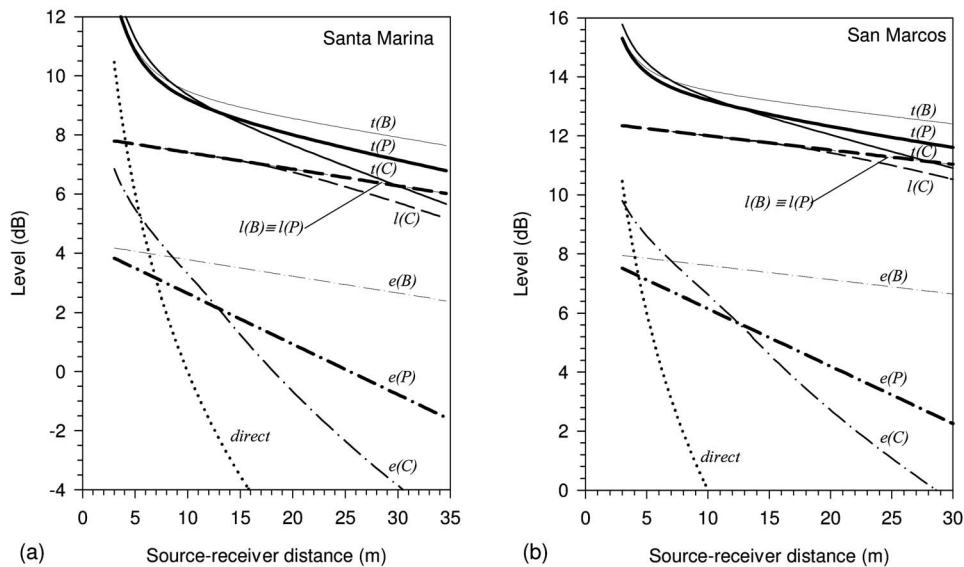


FIG. 12. Dependence for the different temporal energy components (e , early; l , late; t , total), as a function of source-receiver distance, calculated from Barron's model (B), Cirillo's model (C), and the proposed in this work (P), (a) for Santa Marina church, and (b) for San Marcos church.

longer distances than the proposed μ adjustment. For the late reflected energy the three models practically coincide as expected and, for the total energy, Barron's value shows a remarkable overestimation while a notable coincidence for the other two models may be highlighted. It is only at great distances that Cirillo's model presents some additional attenuation (about 0.6 dB at 25 m from the source).

Finally, this method is applied to some churches analyzed by Cirillo and Martellota, although only partial data (1 kHz octave band) of C_{80} are used to obtain the corresponding values of μ parameters as described in Fig. 6. The results for St. Nicholas Basilica in Bari and Lucera Cathedral are shown in Fig. 13, where the experimental data and the predicted values from Cirillo's model and μ model are plotted as a function of source-receiver distance. These partial results suggest the possibility of a generalization of this methodology so that it can be applied to a wide range of architectural typologies whereby a range of values of μ capable of predicting the acoustic energy parameters from basic geometric and acoustic data of the space are provided.

From the presented results it is possible to propose a typological model to evaluate and predict acoustic energy parameters for these religious spaces. The proposal is to use the $\bar{\mu}$ value and its geometric (V) and acoustic (T) characteristics for each church. To this end, Fig. 14 shows the T_S function calculated from this typological model (through Eq. (24) with $\bar{\mu}$ value), those values from their corresponding μ in Eq. (24), and the experimental results versus source-receiver distance, for four churches: San Julián which is in the lower limit of the μ range, Santa Marina and San Esteban which are in the middle range, and San Marcos in the upper limit. Only slight differences appear between the two theoretical lines. The differences found at the farthest point from the source are, 23 ms (11%) at 30 m for San Julián church, 4.4 ms (1.6%) at 35 m for Santa Marina church, 1.9 ms (0.9%) at 25 m for San Esteban church, and 9.6 ms (3%) at 30 m for San Marcos church, respectively.

Consequently, with the calculation of μ coefficients developed in these churches, a relatively simple model based on C_{80} experimental data may be obtained which provides an

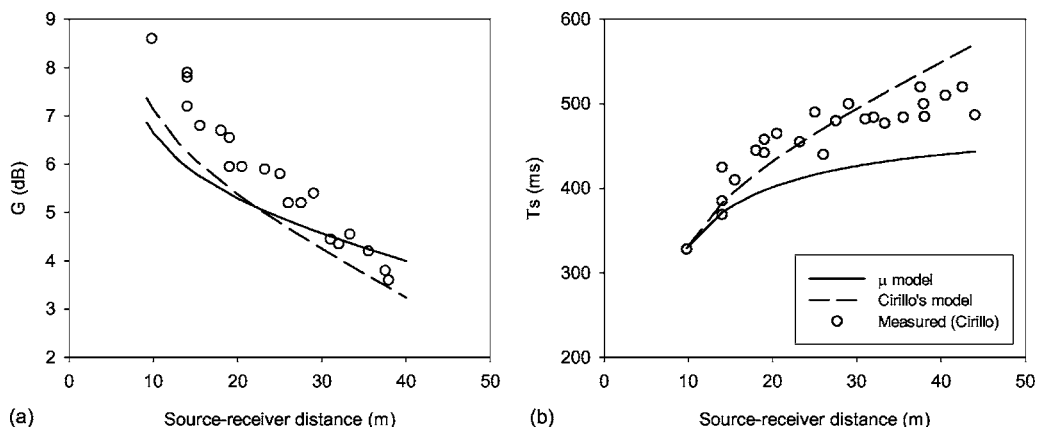


FIG. 13. Measured and predicted values from Cirillo's model and the proposed μ model of G for St. Nicholas Basilica in Bari (a) and of T_S for Lucera Cathedral (b).

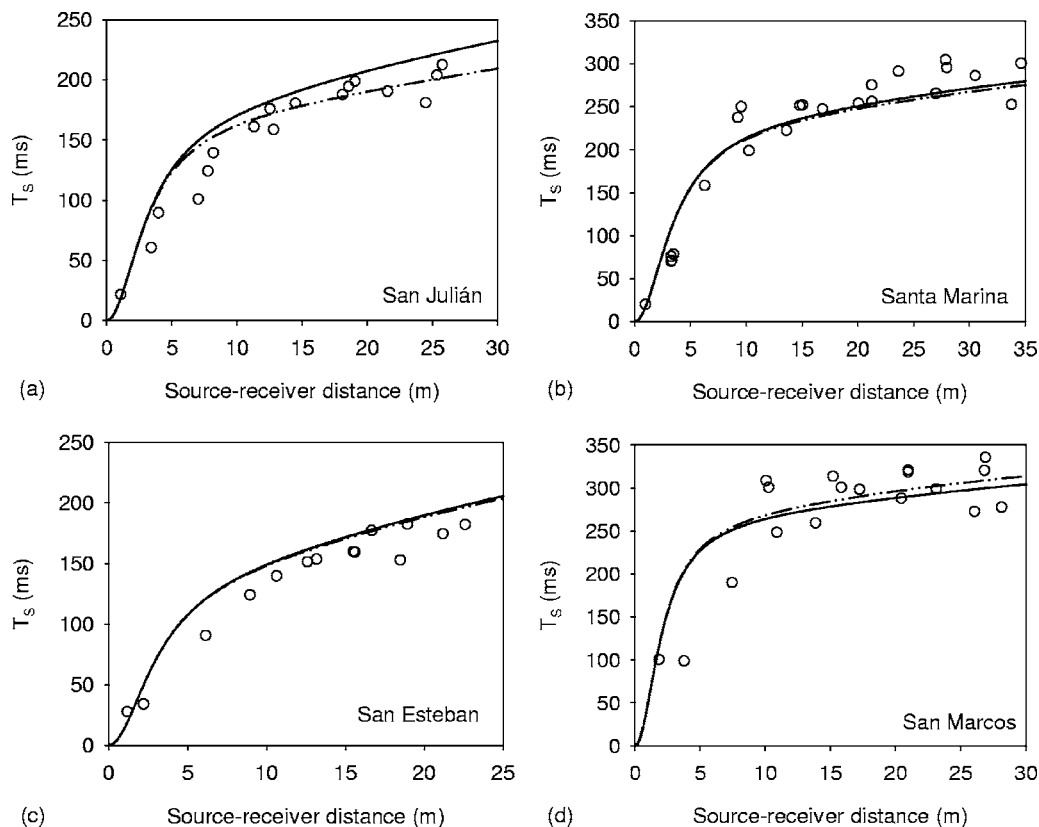


FIG. 14. Comparison of theoretical T_s function calculated from $\bar{\mu}$ (continuous line) and from its μ (dotted line) value, and the experimental results (o) vs source-receiver distance, (a) for San Julián church, (b) for Santa Marina church, (c) for San Esteban church and (d) for San Marcos church.

acceptable prediction of the values of the most important parameters in order to evaluate acoustic quality of rooms based on sound energy criteria. By rigidly maintaining the upper limit of the early energy interval at 80 ms for all reception points, Eq. (23) differs from Cirillo's model which establishes a variable time for each position in which the normalized energy density changes its behavior from linear to exponential. Hence certain difficulties arise for evaluating the early energy for clarity calculations according to the positions of 80 ms time with respect t_R , and although Cirillo's proposal is a very coherent and elegant theoretical model, the procedure developed here avoids these complications and also yields similarly good results in its predictions.

VI. CONCLUSIONS

In the 12 Mudejar-Gothic churches under study an analysis has been undertaken of the most relevant energy-based monaural parameters: clarity, definition, sound strength, and center time, as a function of source-receiver distance. These parameters have been averaged spectrally in the most widely accepted way suggested for concert hall and auditoria in order to describe sound quality. The limitation of the previous adjustment model adopted by Sendra, Zamarreño, and Navarro⁸ for this type of religious building is that it is only capable of justifying the behavior of the total sound pressure level with source-receiver distance. This limitation has been overcome by using the procedure developed in this work. The proposed methodology involved calculating the early energy by adjusting the μ coefficient introduced in the

distance-dependent exponential through nonlinear regression in order to maximize the correlation between the predicted and the experimental values of clarity in these spaces, and by maintaining the late energy expression suggested by Barron's model. The input variable μ , which takes into account the conformation of the boundary surfaces, interior decoration and furniture in those spaces, together with the input variables V , T , and r , enables all the remaining acoustic parameters (definition, sound strength, and center time) to be deduced in these worship enclosures with acceptable accuracy.

The accuracy of the methodology has been checked by comparing spatially averaged measured values for each parameter with those calculated using Barron's model and the proposed model. Likewise, a comparison between mean values of absolute differences for each position in each church has been analyzed. In both cases the results confirm the prevalence of the proposed model for these religious spaces.

From the set of calculated μ coefficients, a typological model is proposed using the $\bar{\mu}$ value and the specific geometrical (V) and acoustic (T) data for each church. This typological model has been verified extensively through the T_s parameter.

The similarity of the predictions for the total early and total temporal components of the energy with Cirillo's model and the one proposed here is remarkable, and although Cirillo's study is a notable theoretical contribution to the insight of sound field in churches, more simple relations are deduced with the typological model proposed in this work.

Finally, it is necessary to mention that the methodology accomplished here may be extended to include other types of closed rooms, thereby indicating a greater prediction potential. This would require more intensive in situ measurement to establish the μ values for different typologies. In order to verify the feasibility of this extension, the μ model methodology has been applied to the churches analyzed by Cirillo and Martellota¹⁰ and, despite only partial data having been used, the results nevertheless point towards the validity of this potential.

ACKNOWLEDGMENTS

The authors would like to thank the priests and church management for allowing the measurements to be carried out. This work has been partially supported by the Spanish MCYT Project No. BIA2003-09306-CO4-02.

- ¹A. P. O. Carvalho, "Influence of architectural features and styles on various acoustical measures in churches," Ph.D. dissertation, University of Florida (1994).
- ²J. J. Sendra, T. Zamarreño, and J. Navarro, "Acoustics in churches," in *Computational Acoustics in Architecture*, edited by J. Sendra (Witpress, Southampton, 1999), pp. 133–165.
- ³A. A. Adel, "Measurement of acoustical characteristics of mosques in Saudi Arabia," *J. Acoust. Soc. Am.* **113**, 1505–1517 (2003).
- ⁴*Proceedings of the 17th International Congress on Acoustics*, CD-ROM Vol. III. Architectural Acoustics: Acoustics of Worship Buildings (14 communications) (ISBN 88-88387-02-1) Rome, Italy, 2–7 September (2001).
- ⁵*Proceedings of the Forum Acusticum*, CD-ROM: ARC Architectural Acoustics: RBA-05: Worship Building Acoustics (16 communications) (ISBN 84-87985-07-6) Seville, Spain, 16–20 September (2002).
- ⁶Z. Karabiber, "A new approach to an ancient subject: CAHRISMA project," on CD-ROM: 4–7 July, *Seventh International Congress on Sound and Vibration*, Garmisch-Partenkirchen, Germany (2000).
- ⁷M. Barron and L. J. Lee, "Energy relations in concert auditoriums I," *J. Acoust. Soc. Am.* **84**, 618–628 (1998).
- ⁸J. J. Sendra, T. Zamarreño, and J. Navarro, "An analytical model for evaluating the sound field in Gothic-Mudejar churches," in *Computational Acoustics and its Environmental Applications II*, edited by C. A. Brevia, J. Kenny, and R. D. Ciskowski (Computational Mechanics, Southampton, 1997), pp. 139–148.
- ⁹E. Cirillo and F. Martellota, "An improved model to predict energy-based acoustic parameters in Apulian-Romanesque churches," *Appl. Acoust.* **64**,

- 1–23 (2003).
- ¹⁰E. Cirillo and F. Martellota, "Sound propagation and energy relations in churches," *J. Acoust. Soc. Am.* **118**(1), 232–248 (2005).
- ¹¹M. Galindo, "La acústica en espacios religiosos católicos: Iglesias Gótico-Mudéjares," ("Acoustics in Catholic worship spaces: Mudejar-Gothic churches"), Ph.D. thesis, University of Seville, Spain (2003).
- ¹²L. G. Marshall, "An acoustic measurement program for evaluating auditoriums based on the early/late sound energy ratio," *J. Acoust. Soc. Am.* **96**, 2251–2261 (1994).
- ¹³W. Ahnert and H. P. Tennhardt "Acoustics for Auditoriums and Concert Halls," in *Handbook for Sound Engineers*, edited by G. M. Ballou (Elsevier, New York, 2005) pp. 109–155.
- ¹⁴I. D. Angulo, "Arquitectura mudéjar sevillana de los siglos XIII, XIV, y XV," ("Sevillian mudejar architecture in the XIIIth, XIVth and XVth centuries"), Ayuntamiento de Sevilla (1983).
- ¹⁵M. Galindo, T. Zamarreño, and S. Girón, "Acoustic analysis in Mudejar-Gothic churches: Experimental results," *J. Acoust. Soc. Am.* **117**(5), 2873–2888 (2005).
- ¹⁶V. O. Knudsen and C. M. Harris, *Acoustical Design in Architecture*, 5th ed. (Acoustical Society of America, New York, 1998).
- ¹⁷A. P. O. Carvalho, "The use of the Sabine and Eyring reverberation time equations to churches," *J. Acoust. Soc. Am.* **97**, 3319 (1995).
- ¹⁸A. Magrini and P. Ricciardi, "Coupling effects in Christian churches: Preliminary analysis based on a simple theoretical model and some experimental results," on CD-ROM: Seville (Spain), 16–20 September, *Proceedings of the Forum Acusticum* (ISBN 84-87985-07-6) (2002).
- ¹⁹A. P. O. Carvalho, "Relations between rapid speech transmission index (RASTI) and other acoustical and architectural measures in churches," *Appl. Acoust.* **58**, 33–49 (1998).
- ²⁰E. Cirillo and F. Martellota, "Acoustics of Apulian-Romanesque churches: Correlations between architectural and acoustical parameters," *Build. Acoust.* **10**(1), 55–76 (2003).
- ²¹A. Magrini and P. Ricciardi, "Churches as auditoria: Analysis of acoustical parameters for a better understanding of sound quality," *Build. Acoust.* **10**, 135–158 (2003).
- ²²L. Cremer, H. A. Müller, and T. J. Schultz, *Principles and Applications of Room Acoustics* (Applied Science, London, 1982), Vol. 1.
- ²³S. Chiles and M. Barron, "Sound level distribution and scatter in proportionate spaces," *J. Acoust. Soc. Am.* **116**(3), 1585–1595 (2004).
- ²⁴M. Vorländer, "Revised relation between the sound power and the average sound pressure level in rooms and consequences for acoustic measurements," *Acustica* **81**, 332–343 (1995).
- ²⁵M. Galindo, T. Zamarreño, and S. Girón, "Clarity and definition in Mudejar-Gothic churches," *Build. Acoust.* **6**, 1–16 (1999).
- ²⁶H. Arau, "General theory of the energy relations in halls with asymmetrical absorption," *Build. Acoust.* **5**(3), 163–183 (1998).
- ²⁷A. C. Gade, "The influence of architectural design on the acoustics of concert halls," *Appl. Acoust.* **31**, 207–214 (1990).